Kinga Brzoza-Malczewska,
***Jarosław Janicki,**
***Czesław Ślusarczyk,**
***Włodzimierz Biniaś,**
****Grzegorz Malczewski**

Institute of Biopolymers and Chemical Fibres,
ul. M. Skłodowskiej-Curie 19/27, 90-570 Łódź, Poland,
E-mail: ibwch@ibwch.lodz.pl

***Institute of Textile Engineering and Polymer Materials, University of Bielsko-Biala,**
ul. Willowa 2, 43-309 Bielsko-Biala, Poland

****Institute of Machine Tools and Production Engineering Lodz University of Technology,**
ul. Stefanowskiego 1/15, 90-924 Łódź, Poland

Research in the Supermolecular Structure and Morphology of Chitosan Applied in the Preparation of Dressing Nonwovens

Abstract
Results of research in the preparation of nonwovens containing chitosan salts used as a binding agent are presented. The supermolecular structure of chitosan salts was assessed by the use of wide angle X-ray scattering (WAXS). The crystallinity degree and crystal dimensions were examined. Morphology was assessed by means of optical microscopy.

Key words: *nonwovens, chitosan, dressing, film, WAXS.*

Introduction

Chitosan and its derivatives belong to polysaccharides, a family of polymers with beneficial biostimulating properties like the ability to accelerate wound healing, ease the reconstruction and vascularisation of tissue, and minimise scars. Unique biological properties included in biocompatibility and biodegradability foster the use of these materials in medicine, primarily in dressings.

Modern dressings are designed to shorten the healing time of wounds by the use of tissue- regenerating additives and by providing a favourable environment around the wound. The demand for dressing devices based on natural materials is steadily increasing. Apart from the basic protective functions, such dressings reveal biostimulating properties leading to a limited use of antibiotics which often cause immunity deficiency and micro-flora disorder. Until quite recently, dressing materials were mostly made of cotton or viscose nonwovens. Traditional dressings like gauze or nonwoven compresses do not exert any antibacterial properties which in the case of exudative wounds necessitates the use of drug additives. Standard materials are modified to meet market requirements. New devices shorten the various phases of wound healing and provide optimal conditions for the regeneration of the damaged tissue.

Commercial dressing materials containing polysaccharides like chitosan, chitin and derivatives are presently offered mainly in Japan and the United States. Fuji Spinning Co., Ltd offers products under the trade name of Chitopol - a polynosic nonwoven covered with chitosan with antibacterial and odour-absorbing properties [1]. Eisai is a manufacturer of the chitin-modified PET nonwovens (Chitipack P^{R}) and a cotton-chitosan nonwoven (Chitopack C^{R}). Unitika produces the chitin dressing Beschitin. The University of Washington Medical Center (USA) has developed a dressing material that regenerates skin after II and III grade burns. Chitosan stimulates the formation of monocytes and inhibits the growth of bacteria and fungi, thus reducing the risk of infection in the wound [5]. From the American patent description there is known a processing of fibres and nonwovens using an aqueous chitosan salt solution which gives the material antibacterial properties [7]. A polypropylene nonwoven modified with chitosan acetate acquired antibacterial properties and increased absorption capacity [18].

Nonwoven dressings prepared by electrospinning from the chitin derivative – di-butyrylchitin improves the proliferation of cells [2, 3]. Also known is the use of chitosan and alginates in the form of gauze, cotton wool, foam or the like in the preparation of haemostatic materials and as an inter-tissue protection against adhesions [6]. The nonwoven dressing materials have so far been made in a multi-stage process by modification of the earlier produced fleece or other textile material. The process involves additional costs stemming from the consolidation of the fleece by needle punching, shrinking or gluing. The use of such materials is restrained as a result of the fleece parameters prior to the consolidation and of the possible irritation action of the applied adhesive.

Results of research in the preparation of nonwovens by a cheap and simple process were presented [19]. A fleece was applied which was glued with a solution of chitosan salt producing nonwovens with antibacterial properties. Mechanical, biological properties and biodegradability of the prepared nonwovens were presented in earlier publications [8, 9]. This paper reports investigations into the supermolecular structure of the modified chitosan salt used for the gluing of the fleece to prepare the medical nonwovens. In order to describe it the wide angle X-ray scattering method was used. The mass content of the crystalline domains was assessed – so called crystallinity degree of the chitosan – and its salts used in the gluing of the fleece. Also the dimensions of the crystallites in the initial chitosan and its salts were estimated. The morphology structure was examined by optical microscopy inspections both in normal and polarized light transmitting the tested samples. The structure array, appearance and defects of the samples were examined.

An objective of the research was to assess the supermolecular and morphological structure of chitosan and modified solutions of chitosan used as the fleece binding agent and their impact on the useful properties of the prepared nonwovens.

Materials and methods

Materials

Chitosan

Supplied by Vanson Halo Source, (USA) the chitosan was used in the research

Brzoza-Malczewska K, Janicki J, Ślusarczyk C, Biniaś W, Malczewski G. Research in the Supermolecular Structure and Morphology of Chitosan Applied in the Preparation of Dressing Nonwovens. *FIBRES & TEXTILES in Eastern Europe* 2012; 20, 6B(96): 154-159.

with varied molecular weight and similar deacetylation degree (DD). The main quality parameters are shown in ***Table 1***.

Card fleece

- Card fleece of viscose fibres. Producer: Institute of Exploitation Technology, Dept. of Textile Machinery Exploitation, Łódź, Surface mass 20 g/m^2 and 50 g/m^2; Thickness 0.25 mm; 0.75 mm
- Polipropylene card fleece, Producer: LENTEX S.A., Lubliniec, Surface mass 20 g/m^2 and 50 g/m^2; Thickness 0.25 mm; 0.75 mm

Other materials

- Acetic acid, pure for analysis, POCh/ Gliwice
- Lactic acid, pure for analysis, POCh/ Gliwice
- Sodium hydroxide pure for analysis, POCh/Gliwice

Research methods

Preparation of modified chitosan salt solutions (pH = 5.5)

To a distilled water suspension (150 cm^3) of the initial chitosan (2.4 g), lactic or acetic acid was added in an appropriate amount to obtain a 0.8% acid solution. Then, 50 cm^3 of distilled water was admixed and the mixture was stirred for 1 hour. 1% aqueous solution of NaOH was dropped in the chitosan solution obtained to reach pH 5.5. Distilled water was added to a total volume of 240 cm^3.

Preparing a film from the chitosan salt solution

The chitosan salt solution prepared as described above was poured onto PTFE plates where the film was formed at 20 ± 1 °C. The prepared film represented the chitosan salt used as a binding agent in the nonwovens. In its pure form, undisturbed by the presence of polypropylene or viscose fibres, it served as a sample for the examination of the structure.

Preparation of the nonwovens

The dressing nonwovens was prepared bya Fullard padding machine using two kinds of fleece made of staple polypropylene and viscose fibres with a surface mass of 20 or 50 g/m^2. The PP or viscose fleece was protected with a mesh (a polypropylene knitwear, 0,38±0,01mm thick , with surface mass of 71.9 ± 2.0 g/m^2) on both sides to prevent a slippage of loose, oriented fibres. The fleece was then immersed in a chitosan solution for 5 minutes. The surplus of the chitosan solution was pressed out at a speed of 1m/min on rollers with a slot of 0.25 mm. The protection meshes removed, the fleece was dried at 40 ± 1 °C [8, 9] for 4 hours.

Table 1. *Physical-chemical parameters of the starting chitosan; M_V – viscometric average molecular mass; DD – deacetylation degree; Pd - polydispersity.*

Symbol of chitosan	M_v, kD	DD, %	Pd, M_w/M_n	WRV, %	Heavy metal content*, %	Ash content**, %
Vanson 01-CISF-1847 (V3)	166	78.9	5.2	101	0.005	0.30
Vanson 01-CISF-1846 (V12)	267	78.3	5.5	117	0.010	0.90
Vanson 01-ASSC-1769 (V14)	849	82.4	3.5	136	0.003	0.48

Analytical methods

Properties of the initial chitosan

- Average viscometric molecular mass was measured by a diluting method [10, 11],
- Deacetylation degree by potentiometric titration [12],
- Polimolecularity by gel chromatography (GPC) [13] ,
- Water retention value WRV [10],
- Content of heavy metals according to standard PN-82/C-84002.15,
- Content of ash according to standard ISO 3451-1:1997.

Investigation of the chitosan salt used as fleece binder by wide angle X-ray scattering (WAXS)

The investigation was carried out with the use of the URD 63 diffraction meter made by Seifert Co with the CuK$_\alpha$ radiation at the following conditions: acceleration voltage - 40 kV, anode current - 30 mA. A nickel filter and a pulse intensity analyzer provided the monochromatic beam. A scintillation counter served as a detector. The diffraction patterns were prepared in the range of the diffraction angle from 4 to 60° by scanning at 0.1° intervals and pulse counting - 20 s.

For the estimation of the crystal phase content (crystallinity degree) in polymers a separation of the experimental diffraction curve into two components is needed – diffraction from the amorphous area – A_a and crystalline area – A_k in the polymer and then, the computing of the surface underneath the curves (A_a and A_k accordingly).

The crystallinity degree was calculated from the equation:

$$x_k = \frac{A_k}{A_k + A_a}$$

where: x_k – crystallinity degree,

A_k – surface under the diffraction curve representing the crystalline area,

A_a – surface under the diffraction curve representing the amorphous area.

The diffraction patterns were analyzed with the use of the Hindeleh and Johnson method [14]. According to the method, the theoretical curve is obtained by the addition of peaks responding to the diffraction in the crystalline and amorphous areas and the background curve. The polynomial of the 3rd order applies to the description of the background; the factors are adopted in the course of optimizing. The crystalline peaks and amorphous halo are defined by the linear Gauss and Cauchy combination. Each of the peaks is defined by 4 parameters: position, height, half-value width and coefficient indicating its share in the shape of the Gauss and Cauchy function. The choice of all parameters is accomplished by minimizing the sum of squares of the deflection between the theoretical and the experimental curve. The entire computing of the diffraction patterns was made by means of the OPTIFIT [15] software in which the minimizing of the algorithm is applied.

The measurement of the width of the diffraction peak was applied in computing the crystalline area size. The method is based on the Scherrer equation:

$$D_{(hkl)} = \frac{K\lambda}{\beta \cos\theta}$$

where:

$D_{(hkl)}$ – average size of the crystalline areas perpendicular to the plane (hkl);

θ – Bragg angle for the plane (hkl);

λ – length of X-ray wave (for CuK$_\alpha$ λ = 1.54 Å);

β – half -value width of the diffraction peak for the plane (hkl) (in radian);

K – Scherrer constant (for polymers =1).

Investigation of the morphology of the binding agent-chitosan salt by optical microscopy

The polarizer–analyzer arrangement of the microscope with the tested sample placed inside enables to observe the effects of light depolarizing caused by specific properties of the sample. Like crystals, objects with certain crystallinity cause depolarization of the light by rotating the polarization plane of the light crossing the tested object; it is demonstrated as a luminescence on a dark ground. Observation in the dark ground was also made. Such configuration of the microscope enables distinguish objects with varied optical density. The objects are visible as fluorescent images on the grain boundary (inhomogeneity) .

Parameters of the equipment arrangement:
Observation and registration of the photo microscopic images were made using a microscope set comprising of:

- Polarizing microscope POLAM P - 113
- Computer image registering system -video camera Panasonic KR-222, computer video chart MIRO and computer server.

The following magnification was applied in the registration: in the polarizing microscope – magnification of camera and microscope – 180×, 370×.

Results and discussion

WAXS measurements indicate an organised structure and a high crystallinity degree in the samples of the initial chitosan. The diffraction patterns were analyzed based on literature data concerning the elemental cell of chitosan [16]. The source indicates the orthorhombic crystal system as typical to chitosan. The elemental cell has the following dimensions: a = 0.824 nm, b = 1.648 nm, c (chain ax) = 1.039 nm. ***Figures 1 – 3*** present WAXS diffraction patterns for chitosan samples V3, V12 and V14. In the patterns three distinct crystal peaks can be seen which, based on the elemental cell dimensions, were identified as stemming from the lattice planes with factors (020), (110) and (130) respectively. Similar results were reported by Garnpimol [17]. The crystallinity degree and size of the crystalline areas perpendicular to the given lattice planes were estimated for selected chitosan samples and its salts. Results are presented in ***Table 2***.

It may be seen that the crytallinity degree of the starting chitosan Vanson is higher than that in the prepared modified chitosan salts in which a drop in crystallinity occurred by about 20 - 60%. A dependence was observed between the average size of the macromolecule and the crystallinity degree in chitosan marked V3 and V12 where the ability to crystalize was inversely proportional to the polymer chain length. The V3 and V14 chitosans though different in molecular mass, have similar crystallinity degree and crystal size. The initial chitosan V12 shows crystallite size as in the V3 and V14 chitosan salts (lactate and acetate). An impact of the physical-chemical structure of the chitosan macromolecules upon the crystallinity degree could be observed. A high polymolecularity of the V3 and V12 chitosan (***Table 2***) hinders high crystallinity. Chitosan acetate shows higher crystallinity than the lactate with slightly lower crystallite size. The higher content of the amorphous phase in the lactate may indicate better water absorption than in the acetate. Transformation of the chitosan into salts (acetate and lactate) resulted in a decrease in crystallinity. Modification of the salts, in which the pH increases by the use of NaOH, causes a widening of the reflexes, therby it influences the crystallite size measured. No relation was noted between the form of the initial chitosan and the crystallinity degree. Chitosans marked V3 and V12 are powder materials while V14 was in flakes; in neither does a relation between the deacetylation degree and crystallinity degree appear (***Table 1***). The deacetylation degree of the various chitosan lots is similar:
V3 – DD = 78.9%;
V12 – DD = 78.3%;
V14 – DD = 82.8%.

The diffraction patterns in ***Figures 1 - 3*** for the starting chitosans V3, V12 and V14 differ in shape, height and width of the singular peaks.

Comparing the patterns, one can note the differences between the crystal structure of the initial chitosan and that of the film made of chitosan salt. The diffraction patterns of the V3, V12 and V14 chitosans have higher and narrower peaks. The patterns of the modified chitosan salts are presented in ***Figures 4 - 6***.

In the V3 and V12 chitosans two peaks are seen stemming from the deflection on the crystal planes of which one is a sharp mineral peak (probably from sodium hydroxide) while the other one underwent a remarkable reduction. Two peaks related to chitosan acetate were also noted by Zhao [20]. On the basis of the WAXS examinations, one may draw the conclusion that the processing of chitosan with acetic acid causes a decrease in the cystallinity degree. A decrease in the crystallinity does not necessarily mean smaller crystallite size. In chitosan acetates V3 and V12 were found smaller crystallites than in the lactates (***Table 2***). Crystallite size is similar in chitosan acetate and lactate V14. This comes from the considerable decrease in the crystal peak (110) at 2Θ~ 11. Together with the shrinking crystallinity degree, the share of the amorphous phase increases, which contributes to a higher water absorption of the polymer, a feature desired in medical dressing. The obtained results suggest that the highest absorption may be expected in chitosan lactate V3Lac and V14Lac. The salt is best suited to use as binder for the nonwovens.

Table 2. *Parameters of supermolecular structure of chitosan estimated by WAXS method.*

Sample	Crystallinity degree	Crystallite size [16]		
	%	$D_{(020)}$, nm	$D_{(110)}$, nm	$D_{(130)}$, nm
V3 (starting chitosan)	62.4	4.2	5.1	4.3
V3 Ac (chitosan acetate)	28.4	1.6	-	2.3
V3 Lac (chitosan lactate)	19.0	2.4	3.3	2.1
V12 (starting chitosan)	43.7	2.8	3.3	4.7
V12 Ac (chitosan acetate)	29.0	1.4	-	1.8
V12 Lac (chitosan lactate)	23.7	2.5	2.3	1.6
V14 (starting chitosan)	59.9	4.1	5.4	4.2
V14 Ac (chitosan acetate)	42.8	3.2	3.6	2.1
V14 Lac (chitosan lactate)	16.2	3.0	4.4	1.6

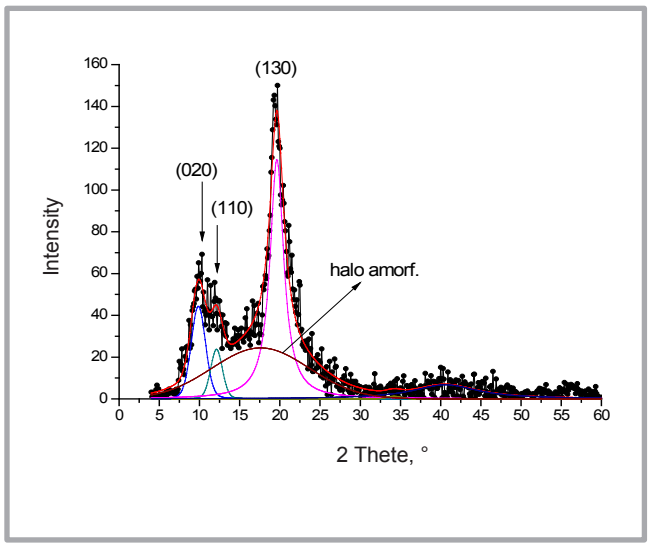

Figure 1. *Diffraction pattern WAXS of the starting chitosan V3. The lattice planes are indicated on the graph.*

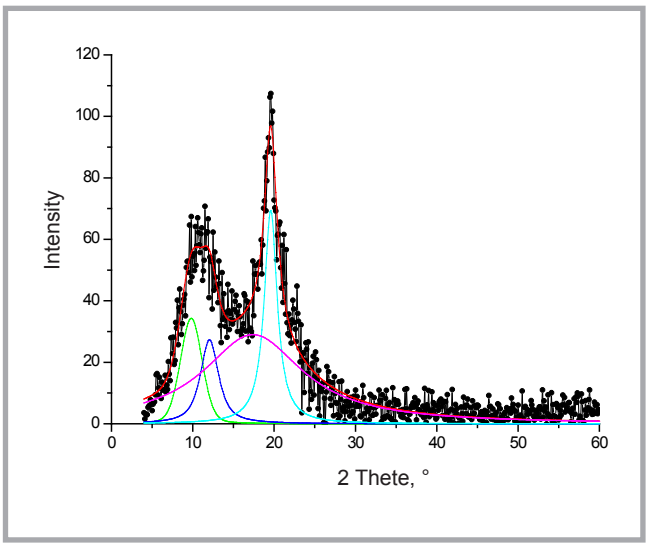

Figure 2. *Diffraction pattern WAXS of the starting chitosan V12.*

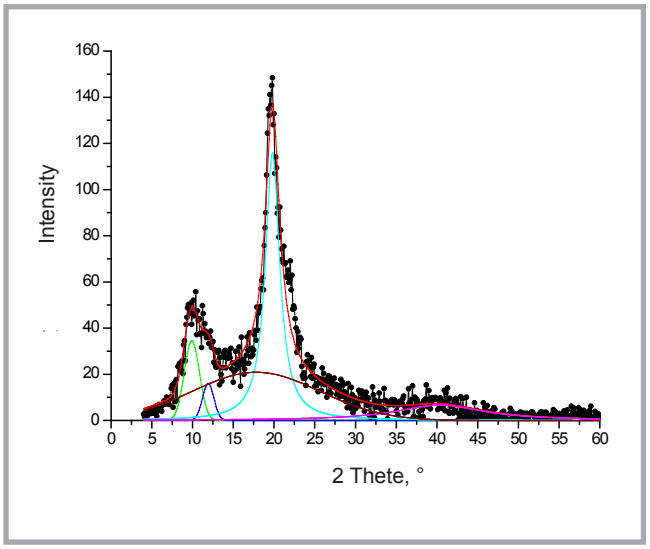

Figure 3. *Diffraction pattern WAXS of the starting chitosan V14.*

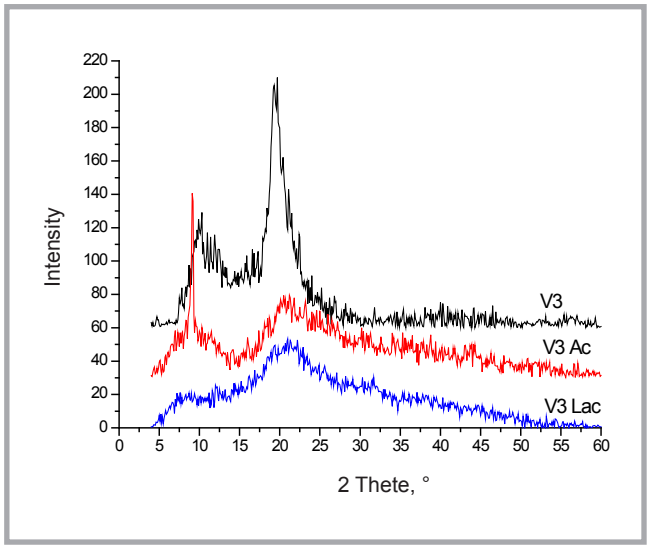

Figure 4. *Comparison of WAXS diffraction patterns of chitosan V3 and its salts-acetate (V3Ac) and lactate(V3Lac).*

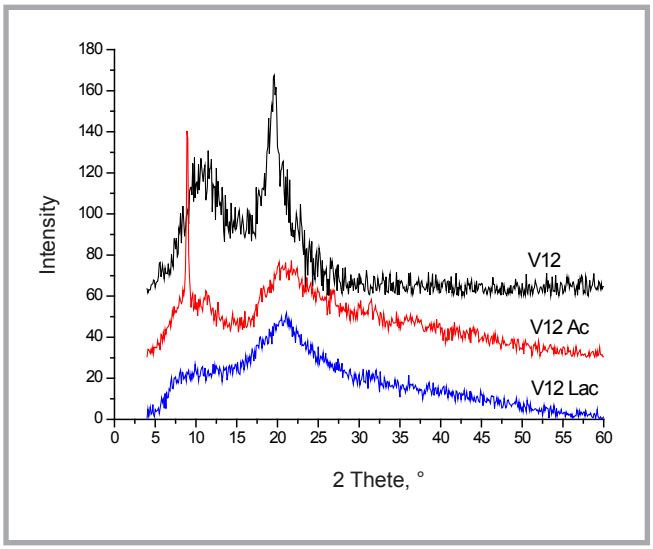

Figure 5. *Comparison of WAXS diffraction patterns of chitosan V12 and its salts-acetate (V12Ac) and lactate (V12Lac).*

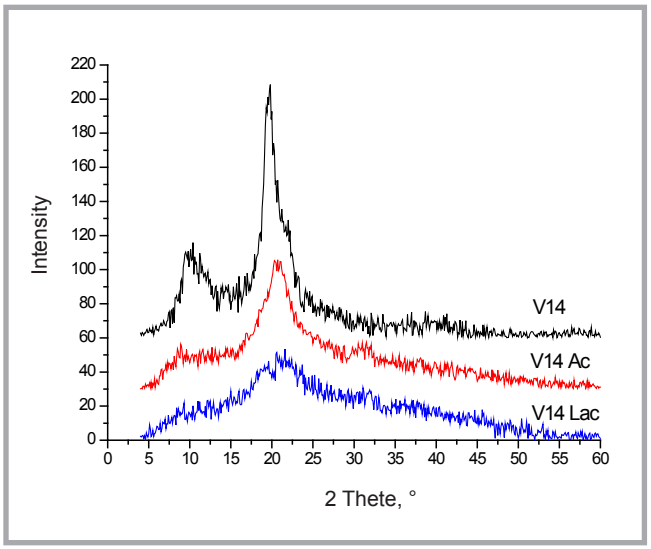

Figure 6. *Comparison of WAXS diffraction patterns of chitosan V14 and its salts-acetate (V14Ac) and lactate (V14Lac).*

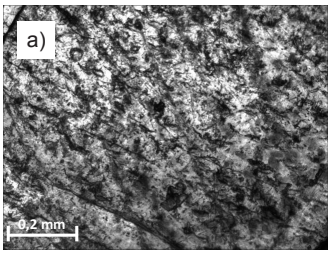

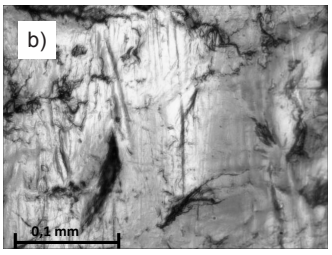

Figure 7. *Image of surface of film made of chitosan salts V3Ac (a), V3Lac (b) in reflected light.*

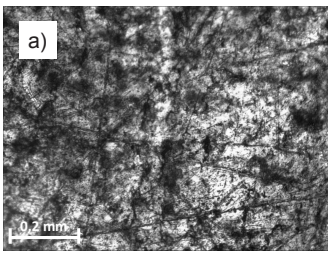

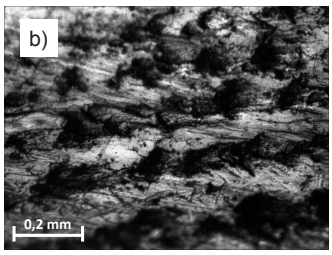

Figure 8. *Image of surface of film made of chitosan salts V12Ac (a), V12Lac (b) in reflected light.*

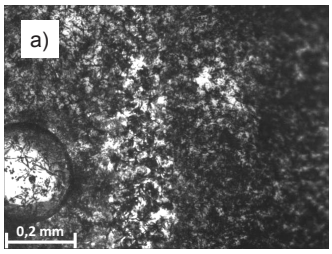

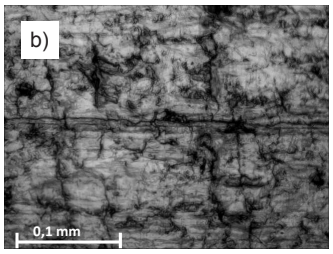

Figure 9. *Image of surface of film made of chitosan salts V14Ac (a), V14Lac (b) in reflected light.*

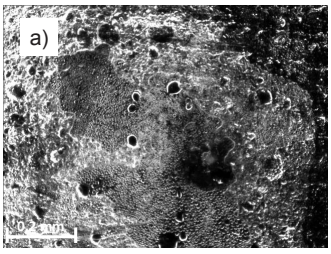

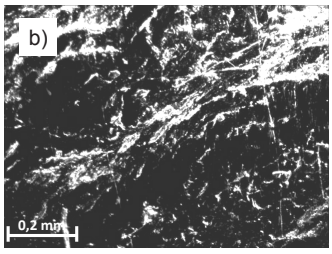

Figure 10. *Microscopic image of film made of chitosan salts V3Ac (a), V3Lac (b) seen in the dark field*

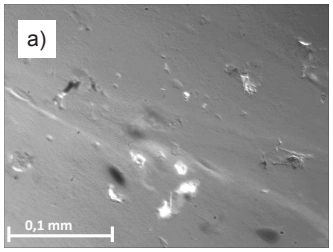

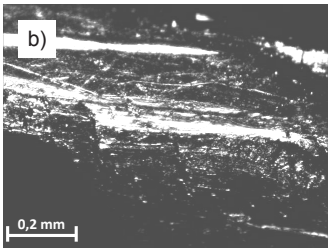

Figure 11. *Microscopic image of film made of chitosan salts V12Ac (a), V12Lac (b) seen in dark field.*

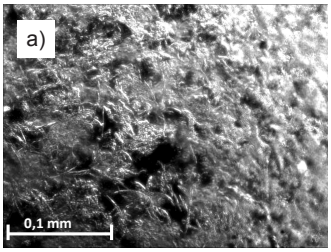

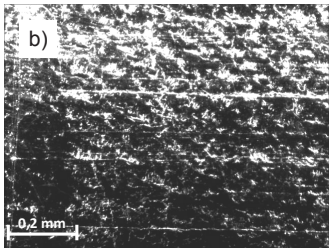

Figure 12. *Microscopic image of film made of chitosan salts V14c (a), V14Lac (b) seen in dark field.*

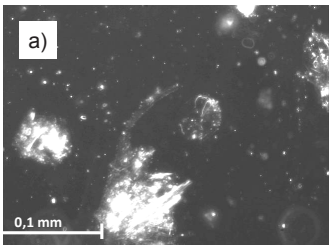

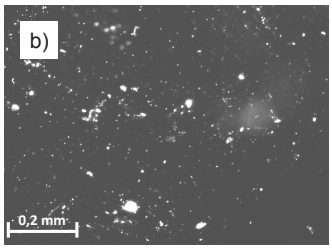

Figure 13. *Microscopic image of film made of chitosan salts V3Ac (a), V3Lac (b) seen in polarized light.*

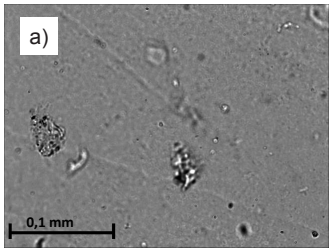

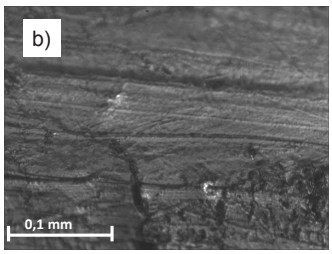

Figure 14. *Microscopic image of film made of chitosan salts V12Ac (a), V12Lac (b) seen in polarized light.*

Microscopic assessment of the morphology structure of the initial chitosan and its salts

The surfaces of film prepared from the chitosan salt V3 with increased pH are uneven with minor cracks. This can be seen in the reflected light images – ***Figure 7.a*** (unevenness) and ***Figure 7.b*** (cracks).

Tiny cracks are also seen in the images of V12 chitosan salt with higher pH (***Figure 8.a***) as well as fine "grains", possibly of CH_3COONa, and surface recesses (***Figure 8.b***)

On the surfaces of film prepared from the chitosan salt V14 with increased pH, numerous tiny cracks are visible (***Figures 9.a, 9.b***). The surface is uneven with characteristic kinks remaining after collapses of the earlier dried outer film surface (***Figure 9.b***).

In the images of film prepared from Chitosan V3 with a higher pH, numerous large objects can be seen with varied optical density (***Figures 10.a, 10.b***), invisible in regular light.

In films made of V12 chitosan salt, a few tiny objects are seen in the dark field with a different optical density (***Figure 11.a***). This is supposedly the effect of the solvent diffusing from the interior after the film surface had solidified leaving ripples and crinkles behind (***Figure 11.b***).

In films prepared from V14 chitosan salt a multitude of objects can be perceived with varied optical density (***Figures 12.a, 12.b***). When solidifying, the V14 salt with the highest molecular mass produces characteristic filiform aggregates that do not appear in other salts. In chitosan V14 the polymer chains are presumably cross-linked by intermolecular bonds hindering complete dissolution

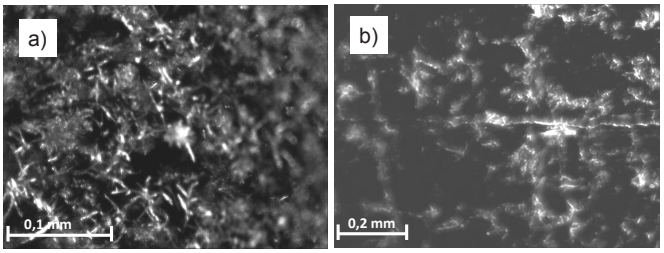

Figure 15. *Microscopic image of film made of chitosan salts V14Ac (a), V14Lac (b) seen in polarized light.*

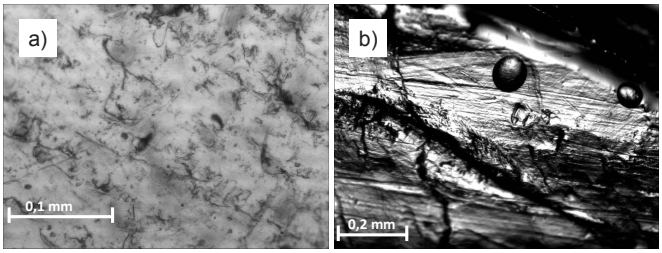

Figure 16. *Microscopic image of film made of chitosan salts V3Ac (a), V3Lac (b) seen in transmitting light.*

and, as a result, causing the precipitation of the said structures

In films prepared from the chitosan salt V3, numerous tiny ordered areas (***Figure 13.b***) can be seen in polarized light as well as bigger crystals (***Figure 13.a***). It may be perceived that the film solidifies in the form of grains; first the longer polymer chains followed by the shorter ones.

In films of the V12 salt, a few small crystals were visible in polarized light (***Figure14.a, 14.b***). The amount of objects luminescing in the polarized light is confirmed by the results of WAXS investigation where chitosan V12 and its salts show a lower crystallinity degree than chitosan V3 and V14. The absence of luminous points may witness a fine-crystal, barely oriented supermolecular structure.

Inspected in polarized light, films made of chitosan salt V14, reveal single tiny objects that in a specific way refract light – they became luminescent and can be easily distinguished from the amorphous phase (***Figure 15.a***). Many somewhat larger ordered areas appear in the film of chitosan acetate (***Figure 15.b***). The crystallite size seen in the photos has no representation in the results of WAXS investigations which showed smaller crystallite size in the investigated salts.

In one of the pictures of films of chitosan salt V14 with higher pH, air bubbles in the film interior can be seen in transmitting light (***Figure 16.b***). High viscosity of the polymer solution from which the film was prepared probably trapped air inside the film. Air bubbles are absent in films made from a solution with lower viscosity (***Figure 16.a***).

Conclusions

It may be noted on the basis of the WAXS investigation that the processing of chitosan with lactic acid causes a major decrease in the crystallinity degree. The lower crystallinity of the chitosan salts is expected to have a beneficial impact upon the absorption capacity of dressing materials containing the salts. The fine crystalline structure of films made of the salts may positively affect the drape ability of the salt-containing dressings.

When films of the modified chitosan salts solidify, a separation of the salts takes place, reflected in an inconsistent optical image. The alleged reason for the separation is the diversified molecular mass of the modified salts. Considering the fine crystalline structure of the films, the uneven array of the crystallites will not remarkably affect tenacity.

Acknowledgment

Special thanks go to Dr M.H Struszczyk for his approval to use the antibacterial nonwovens in the assessment of supermolecular and morphology structure,

References

1. Suzuki Migaku. *Antibacterial composite non-woven fabric* US 5,652,049.
2. Seon Il Jang, Ji Ye Mok, In Hwa Jeon et al., Effect of Electrospun Non-Woven Mats of Dibutyryl Chitin/Poly(Lactic Acid) Blends on Wound Healing in Hairless Mice, *Molecules* 2012; 17: 2992-3007.
3. Blasinska A, Drobnik J., Effects of non-woven mats of Di-O-butyrylchitin and related polymers on the process of wound healing. *Biomacromolecules* 2008; 9(3): 776-82.
4. Muzzarelli RAA. Formulary of wound management products, *Euromed Communication*, 2003
5. Chem In Britain 1994, 39, no. 6, 450.
6. John Thomas Gillison, *An improved surgical material.* GB619165.
7. Christine Wild, Raymond Mathis, Edda Schirmer *Method for providing fibers or non-woven fabric with an antimicrobial finish*. US 6,936,345, 2002.
8. Struszczyk MH, Ratajska M, Brzoza-Malczewska K. *Fibres & Textiles in Eastern Europe* 2007; 15, 2(61): 105-109.
9. Struszczyk MH, Brzoza-Malczewska K, Szalczynska M. *Fibres & Textiles in Eastern Europe* 2007; 15, 5-6(64-65): 163-166.
10. Struszczyk MH, Peter MG, Loth F, *Progress on Chemistry and Application of Chitin and Its Derivatives*, ed. H. Struszczyk, Łódź, Poland 1999, p. 168.
11. Struszczyk MH, Loth F, Peter MG., Analysis of Deacetylation Degree in Chitosans from Various Sources. In: A. Domard, G. A. F. Roberts, K. M. Vårum (eds.), *Advances in Chitin Science*, Vol. II, J. André Publishers, Lyon, 1998, pp. 71-77.
12. Ratajska M, Struszczyk MH, Boryniec S, Peter MG, Loth F. *Polimery*, 1997; 42: 572.
13. Rinaudo M. *J. Biol. Macromol.* 1993; 15: 281-284.
14. Hindeleh AM, Johnson DJ. *J. Phys. D: Appl. Phys*. 1971; 4: 259.
15. Rabiej M. *Polimery* 2002; 6: 423; Rabiej M. *Polimery* 2003; 4: 288.
16. Ogawa K, Hirano S, Miyanishi T, You T, Watanabe T. *Macromolecules* 1984; 17: 973.
17. Garnpimol CR, Thawatchai P, Tamotsu K. *International Journal of Pharmaceutics* 2002; 232: 11–22.
18. Huang K-S, Lian H-S, Chen J-B. *Fibres & Textiles in Eastern Europe* 2011; 19, 3 (86): 82-87.
19. Struszczyk MH, Brzoza-Malczewska K, Pat appl. P. 379046.
20. Zhao J, Han W, Chen H. *Carbohydrate Polymers* 2011; 83: 1541–1546.

Received 16.10.2012 Reviewed 16.11.2012